

Optimal Sizing and Economic Evaluation of Hybrid Photovoltaic/Wind/Battery/Diesel Generation Systems for Autonomous Utilization

Ahmed Yamany¹, Mohamed A. Mohamed^{1,*}, Yehia S. Mohammed¹

¹ Electrical Engineering Department, Faculty of Engineering, Minia University, Minia 61519, Egypt

ARTICLE INFO

Article history:

Received:

Accepted:

Online:

Keywords:

Renewable energy

Optimum sizing

Grey Wolf optimizer

Levelized energy cost

HOMER

ABSTRACT

In this paper, an innovative method is introduced to calculate the optimum size of an autonomous hybrid system to determine the lowest levelized energy cost (LEC) and dummy energy (E_{dummy}) generated from the system with the highest reliability index utilizing an Iterative Optimization Technique (IOT). The system includes photovoltaic (PV) panels, wind turbine generators (WTG), diesel generator (DG) and battery storage. An innovative computer program (CP) has been developed based on real time meteorological data of solar radiation, wind speed, ambient temperature and the load demand of one year in 8,760 hours. An accurate methodology for an autonomous site located in the New Valley Governorate of Egypt and many WTG from different manufacturers for obtaining the maximum energy production at the minimum cost of energy provided by the system has been introduced. The CP modifies the penetration ratio of wind and PV in certain increments to meet the demand load. A validation of the CP is carried out by comparing the acquired results with those obtained from the HOMER software and Grey Wolf Optimizer (GWO). Simulation results showed the effectiveness and simplicity of IOT in determining the optimal size of system.

1. Introduction

With scientific and technological progress, the rapid depletion of fossil fuel resources globally has led to a crucial search for alternative sources of energy to meet daily requirements instead of traditional sources [1]. Renewable energy sources (RES) such as solar and wind has become attractive for energy generation as they are free from pollution, and available all over the world [2]. RES is the most cost-effective solution to solve the problem of power supply shortage in remote areas that do not have access to the utility grid [3]. The need for electricity in these areas is typically met by diesel generator (DG), which creates a great degree of concern due to the high of fuel prices and high levels of pollution in the surrounding environment. In Egypt, solar and wind are the most promising RES utilized [4]. Consequently, many researches and feasibility studies relating to the evaluation of energy potentials and the best allocation of these sources in various areas across the country's territory have been introduced, such as [5-7]. However, a common disadvantage of solar and wind energy is their discontinuous nature and reliance on weather conditions and the differences in solar and wind energy may not correspond to the time distribution of load requirements. Fortunately, the issues resulting from the random nature of RES can be greatly controlled by incorporating two or more sources into an appropriate combination [8].

A hybrid renewable energy system (HRES) that combines solar and wind power units with batteries and DG as a backup can reduce the random and discontinuous nature of each individual renewable power system and help in reducing the energy storage requirements dramatically [9]. Therefore, HRES can be essentially suitable for isolated remote areas. However, some problems result from the increasing complication of the system compared to individual power systems. This complication, caused by the utilization of two or more different sources integrated, makes the sizing and analysis of HRES more difficult [10].

Revised:5 April , 2022, Accepted:10 May , 2022

Many research studies have been investigated in the integration of RES depending on solar and wind resources for energy production. The investigations discover how various variables have effects on the overall performance and the financial feasibility of these systems as introduced in the literature. For example, Ramoji et al. [11] utilized Genetic Algorithm (GA) and teaching learning based optimization to determine the optimum size of a hybrid solar-wind system with battery storage. In their study, the optimization methodology is achieved based on the lowest overall costs of the system components with maximum reliability to provide the load. The outcomes demonstrated that the solar-wind configuration is the most reliable and economical to supply electrical energy for remote area. Tafreshi et al. [12] proposed a methodology for calculating the optimum size of photovoltaic-wind-biogas hybrid system utilizing the GA. The overall cost of the system was the objective function.

Yang et al. [13] suggested a model that composes of three components; PV, WTG and battery bank. The decisions variables used in optimization methodology were the capacity of the PV modules, the WTG units and battery bank in addition to the obtained constraints from weather data and load requirements. The optimum configuration is obtained using loss of power supply probability and the minimum LEC.

Jayachandran et al. [14] proposed an islanded hybrid microgrid system including PV, WTG with batteries for a region in India. The authors used particle swarm optimization (PSO) to obtain the best sizing and configuration of the system components. The reliability under worst-case conditions was assessed and sensitivity analyzes were performed to validate the outcomes. The simulation outcomes show that hybrid microgrid system mainly work with solar and wind energy due to the RES high potential in the region under study.

Eltamaly et al. [15] developed a mathematical model-based-smart grid concept for a hybrid microgrid PV/wind/DG system

with battery storage. The optimum size of the proposed model is determined to obtain the minimum energy cost provided by the system. At the same time, the performance and reliability of the system are improved, through loss of power supply probability.

Mokheimer et al. [16] proposed a methodology to calculate the optimum size a stand-alone hybrid PV/wind system with battery bank. The authors developed a MATLAB code to solve and simulate the mathematical model and performance of the hybrid system with various configurations. The simulation outcomes of the model were validated against the outcomes acquired by HOMER software with an agreement utilizing the real meteorological data of Dhahran in Saudi Arabia.

Mohamed et al. [17] utilized PSO for determining the optimum design of wind/PV hybrid system that depends on the grid. The PSO is utilized for obtaining the lowest cost of the produced energy, in addition to providing electrical energy to local needs and fulfilling specific reliability indicators. In [18], PSO has been utilized for calculating the optimal size of a HRES which consisted of PV, wind, and tidal energy is regarded as a primary energy source with batteries as a secondary energy source. The design objective is to obtain the minimum annual costs of operating the power production system for more than 20 years. In [19], PSO was utilized to obtain the lowest leveled cost of electricity for an isolated hybrid system components. The outcomes showed that the optimal system configuration of the hybrid system included PV, wind, battery, DG and flywheel had a cost of 58.94 ¢/kWh.

Simulated annealing algorithm was utilized in [20] for calculating the optimal size of a hybrid power generation system includes PV/diesel with batteries in order to obtain an optimal balance between the life cycle costs and the emissions from the system. In [21], linear programming method was utilized for calculating the optimum size of solar-wind hybrid system with the lowest mean power generation expenses and meeting the required load reliably.

Grey Wolf Optimizer (GWO) algorithm has been introduced in this paper which is one of the newest swarm intelligence algorithms inspired by the grey wolves in the nature. In [22], GWO was utilized to optimize the configuration of a hybrid energy system that includes PV, DG and battery for a remote rural town called "Djanet" in southern Algeria and determine the overall cost of the system. The simulation results demonstrated the superiority of GWO in determining the lowest cost compared to PSO. Moreover, GWO has been capable of reaching the global optimal with relatively simple computational requirements. In [23, 24], GWO was used to solve economic dispatch problems and showed competitive outcomes in comparison to other famous meta-heuristics methods.

HOMER software was utilized in [25] to optimize an autonomous hybrid system developed mostly on renewable energy, and DG to power a little town in Palestinian domains. The mean energy load of some Residential houses and office buildings is 275 kWh per day. The highest power consumption and mean are 24 kW and 11.4 KW, respectively. The area has considerable potential of solar radiation, with a mean daily level of 5.4 kWh/m² and a mean wind speed 4.22 m/s. The optimization outcomes demonstrated that the most economical configuration is photovoltaic/wind/battery with DG. The total present cost of the hybrid system is US\$491,635. In [26], HOMER software was utilized to optimize the performance of a

hybrid PV/wind/battery system and its Ideal society electricity load in Bangladesh.

From the above mentioned literature, it can be observed that modeling and optimization of the hybrid systems is a promising path for supplying electrical energy, especially for areas deprived of electricity. However, the modeling methodologies of hybrid systems vary from article to another. Also, there is no basic methodology that can provide results with a certain level of reliability. Some mathematical models utilize short-term meteorological data, while others utilize statistical meteorological data to perform and simulate probability density functions or use commercial software only. Moreover, there are limited studies to analyze and model hybrid wind and solar energy systems in Egypt. Therefore, the lack of literature on the modeling of solar and wind systems in Egypt is the motivation for this study.

This paper is aimed to develop a computer program (CP) to optimize the size of a HRES for an autonomous site located in the New Valley Governorate of Egypt using Iterative Optimization Technique (IOT). The HRES is composed of PV, wind, battery and DG. The HRES is designed to supply the load demand as economically as possible and also achieves a certain value of reliability. The methodology is developed to calculate the dummy energy (E_{dummy}) and loss of load probability (LOLP) values in order to obtain the minimum LEC of the system. In the optimization process, the decision variables included are the area of PV panels (APV), the number of WTG (NWTG), battery bank capacity, and DG rated power. Moreover, the state of charge (SOC) of batteries and rated power of DG are designed to ensure that the load can be supplied when the RES generation is insufficient. Finally, the optimum size of the proposed hybrid system with the most economical WTG can be achieved. To validate the proposed technique, comparisons with HOMER and GWO have been performed. The simulation outcomes indicated that the proposed CP can obtain the optimal solution under the specific constraints.

The paper is organized as follows: Section 2 demonstrates the configuration of the hybrid system and the models for the subsystems. The energy management strategies are presented in section 3. The proposed CP based-IOT is demonstrated in section 4. HOMER software and the GWO are presented in Sections 5 and 6, respectively. In section 7, the case study of the selected site location is formulated. In section 8, the simulation results and discussion are presented. Finally, the conclusion is shown in section 9.

2. Hybrid Generating System Modeling

The configuration of the proposed hybrid system is shown in Figure 1. The system includes a PV array, WTG system, battery bank system, DG, bidirectional converter, AC load, and dummy load. The system schematic configuration is simple to realize where the AC load is mainly supplied from the WTG system and PV array through the bidirectional converter. The excess energy produced by the WTG system or/and PV array beyond the load demand is used for charging the battery bank system until it is completely charged. When the battery bank is completely charged, the excess energy is utilized to supply dummy loads such as air-conditioning, heating and pumping water loads. If the energy obtained from the WTG system and PV array is less than

the load demand, the insufficient energy is produced by the battery bank until it is reached the minimum state of charge (SOC_{min}). In case of the battery bank is discharged and the system

cannot satisfy the load, the DG is operated. In the following subsections, the proposed HRES components are modeled in detail.

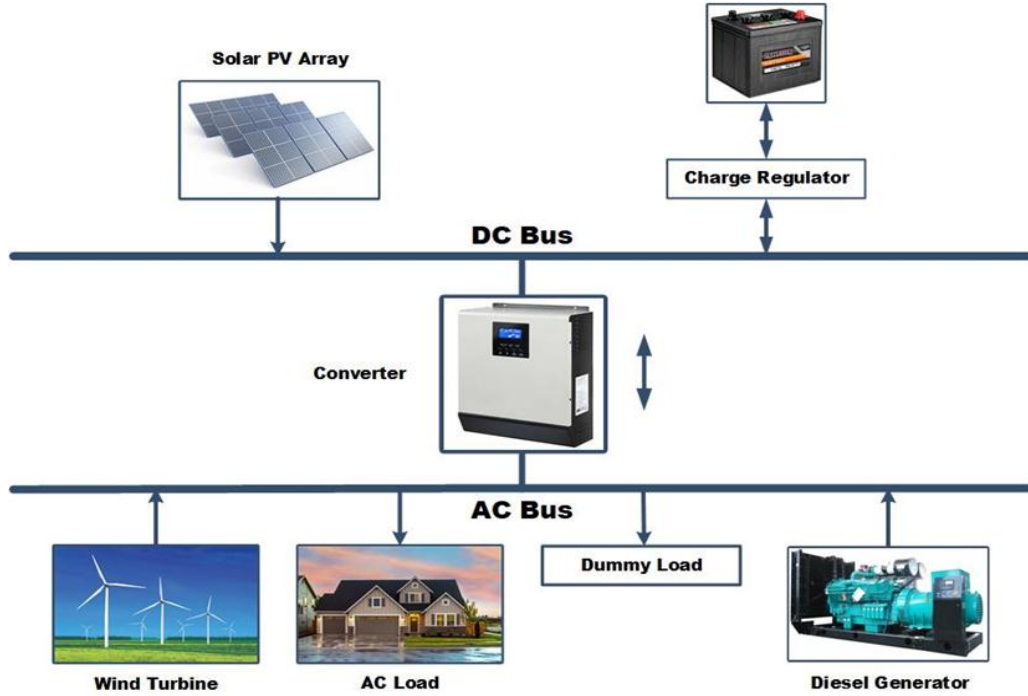


Figure 1: The hybrid system configuration

2.1. Solar PV system model

The power obtained from the PV array system can be determined based on the solar insolation, the PV panel manufacturer data, and the ambient temperature as follows [27]:

$$P_{PV}(t) = G_t(t) \cdot APV \cdot \mu_{pv}(t) \quad (1)$$

where G_t is the solar insolation on the inclined surface and APV is the PV panels area.

The PV module instantaneous efficiency, $\mu_{pv}(t)$ can be calculated from “(2)”:

$$\mu_{pv}(t) = \mu_{th} [1 - K_t (T_c(t) - T_{nom})] \quad (2)$$

where K_t is the temperature coefficient, (K_t is considered 0.0035 per °C for the selected PV module under study). μ_{th} is the solar cell efficiency at standard test conditions (STC), (μ_{th} is considered 20.38% for the selected PV module under study). T_{nom} is the solar cell temperature at STC is often 25°C.

The solar cells temperature at time t , $T_c(t)$ can be determined from “(3)” [28]:

$$T_c(t) = T_{amb} + \left(\frac{NOCT-20}{0.8} \right) G_t(t) \quad (3)$$

where T_{amb} is ambient temperature and $NOCT$ is the nominal operating cells temperature and is considered 45°C for the selected PV module under study.

The area of the PV panels, APV needed to meet the load requirements can be determined as follows:

$$APV = \frac{1}{8760} \sum_{t=1}^{8760} \frac{P_{L,av}(t) S_F}{G_t \mu_{pv}(t) V_F} \quad (4)$$

where $P_{L,av}$ is the required average load, kW. S_F is the factor of safety that considers all possible allowance inaccuracy of insolation recorded data, and in this study the value is 1.1 [29]. V_F is the factor of variability that considers the effects of annual changes in radiation, and in this study the value is 0.95 [29].

2.2. Wind power generator model

The amounts of power generated from a WTG at any area rely on the wind speeds at the hub height. The wind speeds at the height of the WTG hub can be determined utilizing the wind speeds measurements that are taken at anemometer height [30]:

$$v(h) = v(h_g) \left(\frac{h}{h_g} \right)^\alpha \quad (5)$$

where $v(h)$ is the wind speed at the desired height of the hub h -m, m/s. $v(h_g)$ is the wind speed at the height h_g -m, m/s, (h_g is often 10-m). α is the roughness factor was considered in this study as 0.14 [31].

The power obtained from the WTG in each hour can be determined using the subsequent equation [32]:

$$P_W(v) = \begin{cases} 0, & v < v_c \text{ or } v > v_f \\ P_{r_wt} \frac{v^2 - v_c^2}{v_r^2 - v_c^2}, & v_c \leq v \leq v_r \\ P_{r_wt}, & v_r \leq v \leq v_f \end{cases} \quad (6)$$

where P_W is the power obtained from a WTG, kW. P_{r_wt} is the rated electrical power generated from a WTG, kW. v is the wind speed, m/s. v_c , v_r and v_f are cut-in, rated and cut-off wind speeds in m/s, respectively.

The wind speeds data can be statistically analyzed utilizing Weibull distribution to evaluate the wind energy potential at any area as follows [33]:

$$k = a, \quad c = \exp(-b/k) \quad (7)$$

where

$$a = (\sum_{i=1}^w (x_i - \bar{x}) \sum_{i=1}^w (y_i - \bar{y})) / \sum_{i=1}^w (x_i - \bar{x})^2 \quad (8)$$

$$b = \bar{y}_i - a \bar{x}_i = \frac{1}{w} \sum_{i=1}^w y_i - \frac{a}{w} \sum_{i=1}^w x_i \quad (9)$$

$$y_i = \ln(-\ln(1 - F(v_i))), \quad x_i = \ln(v_i) \quad (10)$$

Table 1: The WTG characteristics

	Fuhrlander-3	Ecotecnia-2	ITP-1	NEPC-3	Enercon-2
Cut-in speed, (m/s)	2.5	4	3	4	3
Rated speed, (m/s)	15	14.5	12	15	13
Cut-off speed, (m/s)	25	25	25	25	34
WTG rated power, (kW)	250	600	250	400	330
Rotor diameter, (m)	50	44	30	31	33.4
Hub height, (m)	42	45	50	36	37

2.3. Battery bank model

In accordance with the balance of energy between the PV energy system, the WTG system and the required loads, the state of charge (SOC) of the battery storage can be determined after a specific time (t) using the subsequent equations:

- In charging mode,

$$C_{bat}(t) = C_{bat}(t-1)(1-\sigma) + \left(\frac{P_W(t) - P_L(t)}{\eta_{conv}} + P_{PV}(t) \right) \times \eta_{CH} \quad (14)$$

- In discharging mode,

$$C_{bat}(t) = C_{bat}(t-1)(1-\sigma) - \left(\frac{P_L(t) - P_W(t)}{\eta_{conv}} - P_{PV}(t) \right) / \eta_{DIS} \quad (15)$$

where C_{bat} is the stored energy in the battery. η_{CH} and η_{DIS} are the battery efficiency during charging and discharging (in this article they are taken, 90% and 85%, respectively) [34]. σ is the self-discharge rate of battery and in this article it is considered as 0.2% per day [10]. η_{conv} is the efficiency of converter (in this study it is taken 95%).

The battery must always comply with the following constraints all the time:

$$C_{bat_min} \leq C_{bat}(t) \leq C_{bat_max} \quad (16)$$

where k is the shape parameter and C is the scale parameter, m/s. v_i is the wind speed at time interval i , m/s. w is the number of non-zero wind speeds. \bar{x} and \bar{y} are the average values of x_i and y_i .

For each WTG, the capacity factor can be determined from the following formula:

$$C_F = \frac{\exp[-(v_c/c)^k] - \exp[-(v_r/c)^k]}{(v_r/c)^k - (v_c/c)^k} - \exp[-(v_f/c)^k] \quad (11)$$

The WTG average power output (P_{W_av}) can be estimated as

$$P_{W_av} = C_F \times P_{r_wt} \quad (12)$$

The WTG average number needed to provide the load requirements can be determined through the subsequent equation:

$$ANWTG = \frac{P_{L_av}}{P_{WT_av}} \quad (13)$$

In this paper, Five WTG from various manufacturers has been utilized. Table 1 depicts the characteristics of WTG [27].

$$C_{bat}(t) = C_{bat}(t-1)(1-\sigma) \quad (17)$$

where C_{bat_min} and C_{bat_max} are the minimum and maximum battery bank allowable capacity, respectively.

Moreover, C_{bat_min} can be calculated using the subsequent equation:

$$C_{bat_min} = (1 - DOD) * C_{bat_r} \quad (18)$$

where DOD is the maximum depth of discharge and C_{bat_r} is the battery bank nominal capacity.

2.4. Diesel generator system model

DG is integrated into HRES as a backup to provide the power shortages that cannot be met by PV, WTG and battery systems. The DG consumption of fuel per hour can be evaluated using "(19)" [35]:

$$F(t) = \alpha_{DG} P_{DG}(t) + \beta_{DG} P_{DG,r} \quad (19)$$

where $F(t)$ is DG fuel consumption per hour, L/h. P_{DG} is hourly power produced by the DG, kW and $P_{DG,r}$ is the rated output power of the DG, kW. α_{DG} and β_{DG} are the coefficients of the DG fuel consumption curve, L/kWh, and they were taken as 0.246 and 0.08145, respectively [36].

2.5. Modeling of system reliability

Since the intermittent nature of wind speeds and solar radiation have a great effect on the produced power and cannot meet the required load. Therefore, the reliability analysis of the HRES is regarded as a significant point in the design process for any system as calculated in “(20)”[37]:

$$LOLP = \frac{\sum_0^t \text{Deficit Load Time}}{8760} 100\% \quad (20)$$

where, t is the period of operation for one year in hourly time steps, so $t=8760$.

2.6. Modeling of system cost

LEC is one of the most famous and widely used indicators in HRES economic approach, and can be calculated as follows [10]:

$$LEC = \frac{NPC \times CRF(i,Y)}{ARL} \quad (21)$$

where NPC is the net present cost of the overall project, ARL is the annual required load, and CRF is the capital recovery factor.

CRF can be determined from the subsequent equation:

$$CRF(i, Y) = \frac{i(1+i)^Y}{(1+i)^Y - 1} \quad (22)$$

where Y is the lifetime of project in years and in this article is chosen to be 25 years. The real net rate of interest, i can be calculated from the subsequent equation [10]:

$$i = \frac{i' - f}{1 + f} \quad (23)$$

where i' is the annual nominal rate of interest, and in this paper is used by 8.25% [38]. f is the annual inflation rate, and in this paper is used by 4.9% [39].

The NPC can be calculated using the subsequent equation [29]:

$$NPC = IC + OM + RC + FC - PSV \quad (24)$$

where the initial capital cost, IC , of each part of the HRES, and can be determined through equation “(25)” [29]:

$$IC = C_{PV} \times PV_r + C_{WTG} \times P_{r_wt} \times NWTG + C_{bat_r} \times C_{BT} + P_{r_conv} \times C_{conv} + P_{Dg_r} \times C_{dg} \quad (25)$$

Table 2: The techno-economic parameters of each component of HRES

	PV (kW)	PV civil work (kW)	WTG (kW)	WTG civil work (kW)	Converter (kW)	DG (kW)	Battery (kWh)
IC (\$)	1150	460	1500	300	300	350	220
RC (\$)	Null	Null	1200	Null	270	350	176
OM (%)	1	1	3	3	Null	3	3
Lifetime (year)	25	25	20	25	10	10	4
SV (%)	10	20	20	20	10	20	20
No. of replacements	0	0	1	0	2	2	6
Salvage times	1	1	2	1	3	3	7

3. Energy Management Strategies

where C_{PV} is the cost of PV system including civil works per kW, \$/kW, PV_r is the PV array rated power, kW, C_{WTG} is the cost of WTG including civil works per kW, \$/kW, $NWTG$ is the number of WTG, C_{BT} is the cost of battery bank per kWh, \$/kWh, P_{r_conv} is the rated power of the converter, \$/kW, C_{conv} is the cost of converter per kW, \$/kW, and C_{dg} is the cost of DG per kW, \$/kW.

The operation and maintenance cost, OM , of each component of the HRES during the project life cycle period, which can be determined through the subsequent equation [40]:

$$OM = \sum_{j=1}^Y OM(1) \times \left(\frac{1}{(1+i)^j}\right) \quad (26)$$

The replacement cost, RC , of each component of the HRES during the system life cycle period can be determined through the subsequent equation [40]:

$$RC = \sum_{j=1}^{N_{Rep}} \left(C_{RC} \times C_U \times \left(\frac{1}{1+i}\right)^{Y*j/(N_{Rep}+1)} \right) \quad (27)$$

where C_{RC} is the replacement components capacity, C_U is the replacement components costs, and N_{Rep} is the number of replacements for the system components during Y .

The fuel cost of DG, FC , can be evaluated through the subsequent equation [27]:

$$FC = F(t) t_{dg} P_{fuel} \quad (28)$$

where t_{dg} is the DG overall hours of operation during the life cycle period, h , and P_{fuel} is the price of fuel per liter, (The price of fuel is taken 0.8 \$/L in this study). The present scrap value, PSV , is the estimated cost of the system in the last year of its useful life and can be determined from “(29)” [40]:

$$PSV = \sum_{j=1}^{N_{Rep}+1} SV \left(\frac{1}{1+i}\right)^{Y*j/(N_{Rep}+1)} \quad (29)$$

where SV is the scrap value of the project components.

The techno-economic parameters of each component of HRES are listed in Table 2. This table provides a summary of the IC , OM , RC , PSV , and useful life of HRES components. The cost of the components was estimated taking into account current market prices [41, 42].

Energy management is a methodology utilized to calculate the optimum size of HRES to satisfy the required load. The proposed

methodology is depend on the balance of energy between the generated energy every hour from the system and the load demand, which has been described in-depth in the following subsections:

3.1. Operation methodology

The operation methodology utilized for power operation in the HRES must be recognized at the design step in order to develop an energy balance model and make it correspond to the actual balance of energy. The logic utilized in the operation methodology is summarized as follows:

- If $[P_W(t) > P_L(t)]$ and $[SOC < C_{bat_max}]$, then charging the batteries “(14)” with the excess power $P_{BC}(t) = [(P_W(t) - P_L(t))\eta_{conv} + P_{PV}(t)]\eta_{CH}$. In case of $[SOC \geq C_{bat_max}]$ then stop charging batteries and the excess power is fed the dummy load $P_{dummy}(t) = [(P_W(t) - P_L(t)) + P_{PV}(t)\eta_{conv}]$.
- If $[P_W(t) < P_L(t)]$ and $[P_W(t) + (P_{PV}(t)\eta_{conv})] > P_L(t)$ and $[SOC < C_{bat_max}]$, then charging the batteries “(14)” with the excess power $P_{BC}(t) = [P_{PV}(t) - \frac{(P_L(t) - P_W(t))}{\eta_{conv}}]\eta_{CH} * \eta_{conv}$. In case of $[SOC \geq C_{bat_max}]$ then stop charging batteries and the excess power is supplied the dummy load $P_{dummy}(t) = [(P_W(t) + P_{PV}(t)\eta_{conv}) - P_L(t)]$.
- If $[P_W(t) + (P_{PV}(t)\eta_{conv})] < P_L(t)$ and $[SOC > C_{bat_min}]$ then discharging the batteries “(15)” to cover the load demand with deficit power $P_{BD}(t) = \frac{[P_L(t) - P_W(t) - (P_{PV}(t)\eta_{conv})]}{\eta_{conv}\eta_{DIS}}$.
- If $[P_W(t) + (P_{PV}(t)\eta_{conv})] < P_L(t)$ and $[SOC \leq C_{bat_min}]$, then DG is utilized to secure the deficit in the load $P_{Dg}(t) = [P_L(t) - P_W(t) - P_{PV}(t)\eta_{conv}]$
- If $[P_{Dg}(t) > P_{Dg,r}(t)]$, then the value of $LOLP$ will be increased by one $LOLP = LOLP(t) + 1$.

3.2. Optimization methodology

The aim of the size optimization methodology is the maximization of reliability of the HRES. $LOLP$ is utilized in this study as a technical factor to estimate the system reliability, which considered in this article to be less than 5%. Another aim is the minimization of E_{dummy} and allows it to be exploited to

supply dummy load, which considered in this article to be less than 4% of the required annual load, ARL . Finally, the third aim is to obtain the lowest cost of energy obtained from the system, which is expressed by LEC .

The proposed methodology is utilized to ensure that the annual energy obtained from the system must meet the required load; if not, the capacity of the WTG system and/or PV system must be incremented with a specific amount. Conversely, in case of the annual energy obtained from the system is higher than the load demand, the size of the WTG and/or PV must be decreased with a specific amount. This loop has been repeated every whole year till the annual energy provided by the system is quite satisfying the required load and fulfills the predefined constraints. This logic can be expressed using the following points:

- If $E_{dummy} > 4\%$, then decrease $NWTG$ and APV .
- If $LOLP > 5\%$, then increase $NWTG$ and APV .

When $E_{dummy} < 4\%$ and $LOLP < 5\%$, the optimal size of the hybrid system parts can be achieved. The second stage after optimizing the size of HRES components is calculating the LEC .

In this paper, the proposed methodology utilizes annual hourly meteorological measured data of solar insolation, wind speeds, and temperature at the certain site under study. Moreover, the data of five WTG from various manufacturers have been utilized. The proposed methodology modifies the penetration ratio, which is the ratio of WTG system to the overall power generated from RES with 5% steps to supply the required load for the selected site under study. The optimal penetration ratio is obtained based upon the lowest LEC .

4. Computer Program Based-IOT

Based on the methodologies demonstrated above, a CP is applying using the IOT to size and optimize each component of HRES, which allows simulating the system through calculating the balance of energy for every hour of the year.

The CP can optimize the size of each HRES part based upon the lowest cost of produced energy, LEC . Also, the CP can select the best WTG for the specific location. The CP was developed in flexibly manner using MATLAB code. The CP can change the constraints values and parameters of optimization such as E_{dummy} , $LOLP$. The flowchart describing the CP is shown in Figure 2.

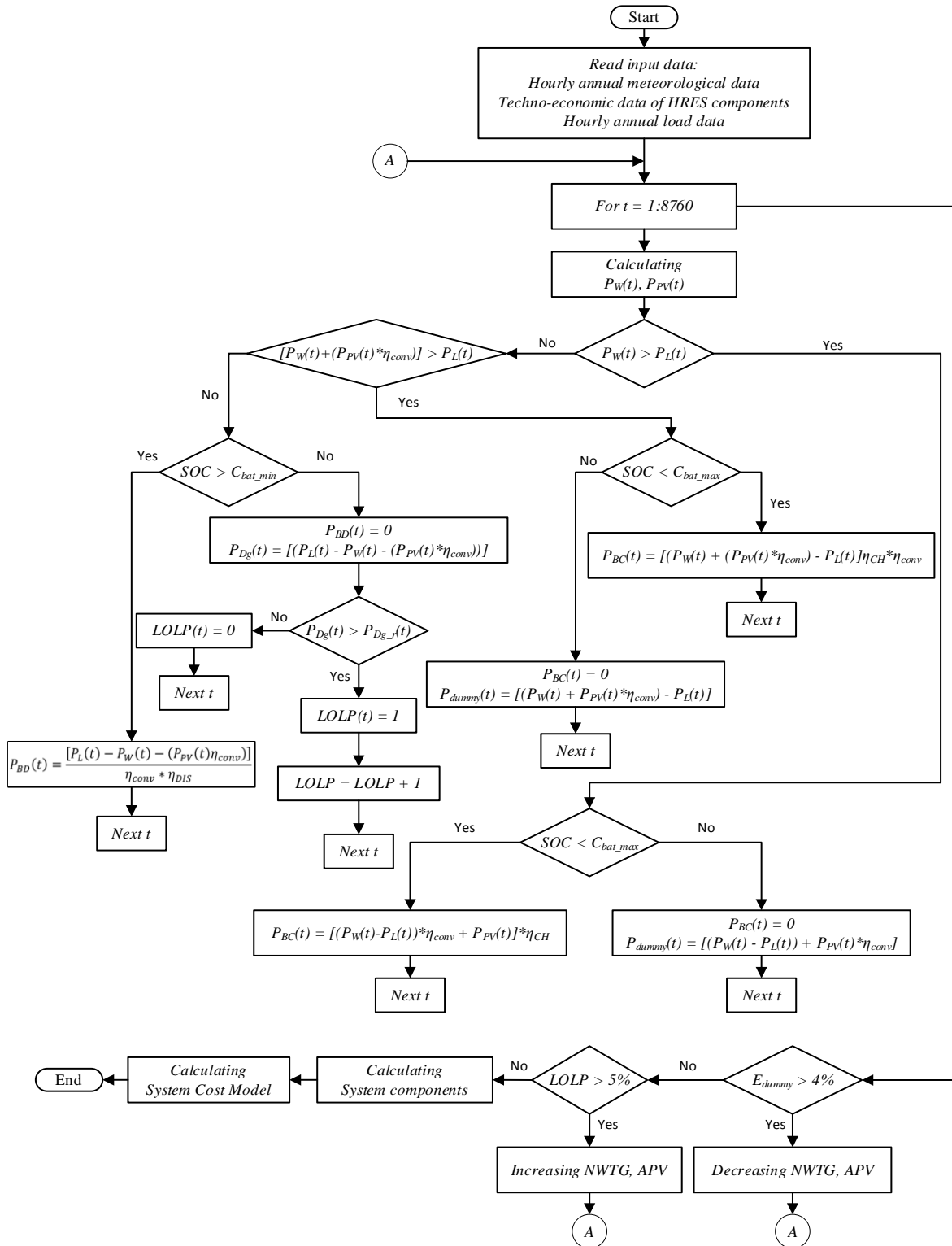


Figure 2: The flowchart of the CP

5. HOMER Simulation Software

The HOMER is a computer software model that was designed by the US National Renewable Energy Laboratory (NREL). The HOMER software has been developed to enable in the designing of the HRES and to simplify the comparison between several

power production technologies in a variety of applications. The physical behavior of the systems and its life cycle costs can be modeled with HOMER software.

HOMER can perform a detailed economic calculations that taking into account all financial factors, however the designated

calculations are not displayed, and it is only like a black box with a restricted flexibility to change the input data without being able to change or check the methods used to perform the economic modeling. In addition, this software has another shortfall: the software cannot calculate the optimum size of the HRES components, but it can only utilize the decision parameters that the modeler specifies into the software to select one of those options.

6. Grey Wolf Optimizer

The GWO algorithm has been first proposed by Mirjalili and Lewis in the year 2014. The GWO is a promising optimization technique which is inspired by the grey wolves in the nature and simulates the hierarchy of leadership and the hunting behavior of the grey wolves. As mentioned in the literature [22-24], GWO showed competitive outcomes in comparison to other famous meta-heuristics methods. GWO has several advantages, including flexibility, simplicity, high performance, and the avoidance of local optima. It is also simple to apply and just has a few control variables to initiate. The four kinds of grey wolves like alpha (α), beta (β), delta (δ), and omega (ω) are used to simulate the leadership hierarchy as shown in Figure 3 [43].

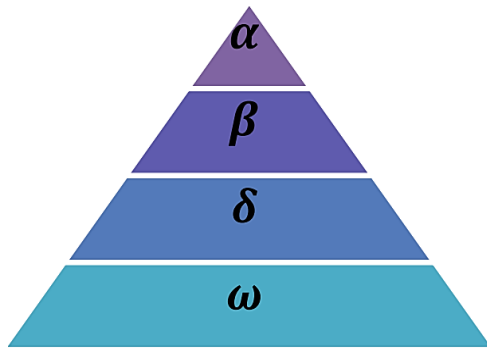


Figure 3: The grey wolf leadership hierarchy

The leaders are referred to as alpha, which is principally liable for choices, making like hunting, waking time, sleeping places, etc. Although, the pack is subjected to the commands of alpha, some form of democratic behavior has likewise been noticed, where an alpha follows different wolves in the pack. The alpha wolves are additionally called the dominant wolves as the pack must follow their orders. The beta is the second level in the grey wolf hierarchy which is subordinate wolves. Beta aids the alpha wolves in taking of decisions or other activity of the pack. The beta wolves could be a male or a female, and are likely the best candidates to become the alpha if any of the alpha wolves die or become very old. The omega is the lowest ranked grey wolves, which are considered as a scapegoat [43].

The technique of hunting and the social leadership of the grey wolf must be mathematically modeled in order to implement the GWO algorithm and calculate the optimum size of the HRES and estimate the lowest *LEC* generated from the system.

It has been considered that the best solution is named alpha (α). Therefore, the second best solution is beta (β) and the third best solution is delta (δ). The remainder of the candidate solutions is supposed to be omega (ω). The hunting (optimization) process

in the GWO algorithm is driven by α , β and δ . The ω wolves follow these three wolves in search of the global optimal solution. Moreover, the social hierarchy, the following equations have been supposed to simulate the grey wolves encircle behavior while hunting [43]:

$$\vec{D} = |\vec{C} \cdot \vec{X}_p(t) - \vec{X}(t)| \quad (30)$$

$$\vec{X}(t+1) = \vec{X}_p(t) - \vec{A} \cdot \vec{D} \quad (31)$$

where \vec{X} is the grey wolf position, \vec{X}_p is the prey position vector, and t is the current iteration number.

\vec{A} , \vec{C} are coefficient vectors that can be calculated by the subsequent equations:

$$\vec{A} = 2\vec{a} \cdot \vec{r}_1 - \vec{a} \quad (32)$$

$$\vec{C} = 2\vec{a} \cdot \vec{r}_2 \quad (33)$$

where \vec{a} is assumed to be linearly decreased from 2 to 0 through the process of iterations, and \vec{r}_1 , \vec{r}_2 are random vectors from 0 to 1.

The grey wolves are able to identify the prey location and encircle it driven by the alpha, but in the abstract search space, the position of the optimal solution (prey) is unknown. Consequently, with the aim of mathematical simulation of hunting mechanism of the grey wolves, it has been supposed that alpha, beta and delta known additional knowledge about the possible location of the prey. Based on that the first three best solutions as yet will be saved and the other search agents like omega that have to update their locations depending on the three currently best locations. The proposed process can be mathematically modeled with the following update equations:

$$\vec{D}_\alpha = |\vec{C}_1 \cdot \vec{X}_\alpha - \vec{X}| \quad (34)$$

$$\vec{D}_\beta = |\vec{C}_2 \cdot \vec{X}_\beta - \vec{X}| \quad (35)$$

$$\vec{D}_\delta = |\vec{C}_3 \cdot \vec{X}_\delta - \vec{X}| \quad (36)$$

$$\vec{X}_1 = \vec{X}_\alpha - \vec{A}_1 \cdot (\vec{D}_\alpha) \quad (37)$$

$$\vec{X}_2 = \vec{X}_\beta - \vec{A}_2 \cdot (\vec{D}_\beta) \quad (38)$$

$$\vec{X}_3 = \vec{X}_\delta - \vec{A}_3 \cdot (\vec{D}_\delta) \quad (39)$$

$$\vec{X}(t+1) = \frac{\vec{X}_1 + \vec{X}_2 + \vec{X}_3}{3} \quad (40)$$

The search agents can update its location based on alpha, beta, and delta as shown in Figure 4 in a two-dimensional search space [43]. In addition, it can be seen that the final position will be at a random location within a circle defined by the alpha, beta and delta positions in the search space.

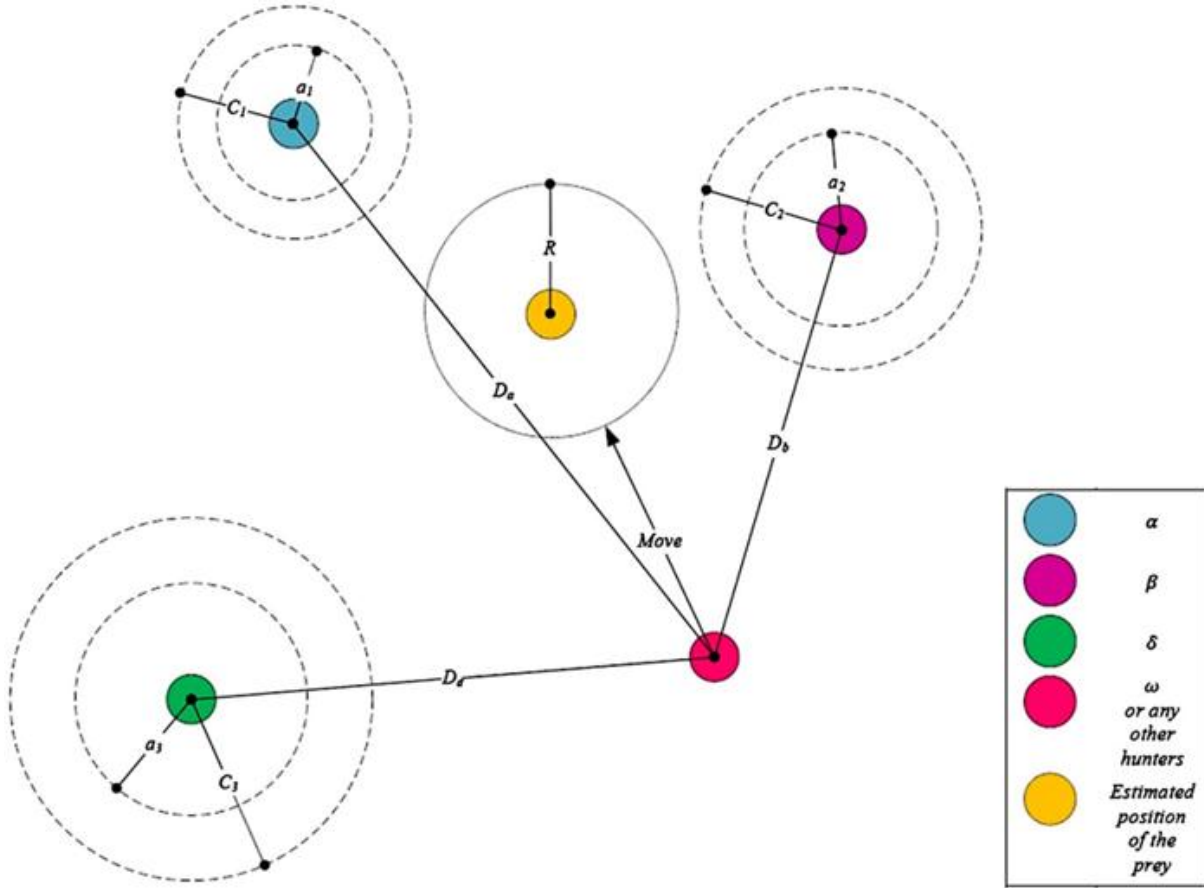


Figure 4: The GWO location updating

When the prey no longer moves, the grey wolves will attack it and the hunting mechanism is finished. For the purpose of mathematically modeled this process the value of \vec{a} is decreased from 2 to 0, which also decreases the value of \vec{A} . In case of the values of \vec{A} lie in $[-1, 1]$, the grey wolves will attack the prey. The vector \vec{C} is another GWO component which can favor exploration. The \vec{C} have random values in the interval $[0, 2]$, that will provide random weights of the prey so as to stochastically emphasize ($C > 1$) or deemphasize ($C < 1$) the effect of prey in determining the distance in the “(30)”.

In order to perform the energy management methodology as well as the procedures of optimization for the hybrid system, a CP depend on GWO has been designed, which was carried out in flexibly manner using MATLAB code that is not able to be done with commercially widely used software, like HOMER. The proposed GWO program can calculate the optimum size of the hybrid system to provide the load requirements with the lowest LEC from the most economic WTG and satisfy the permitted limits for $LOLP$ and E_{dummy} . The process of optimization using GWO algorithm is shown in Figure 5.

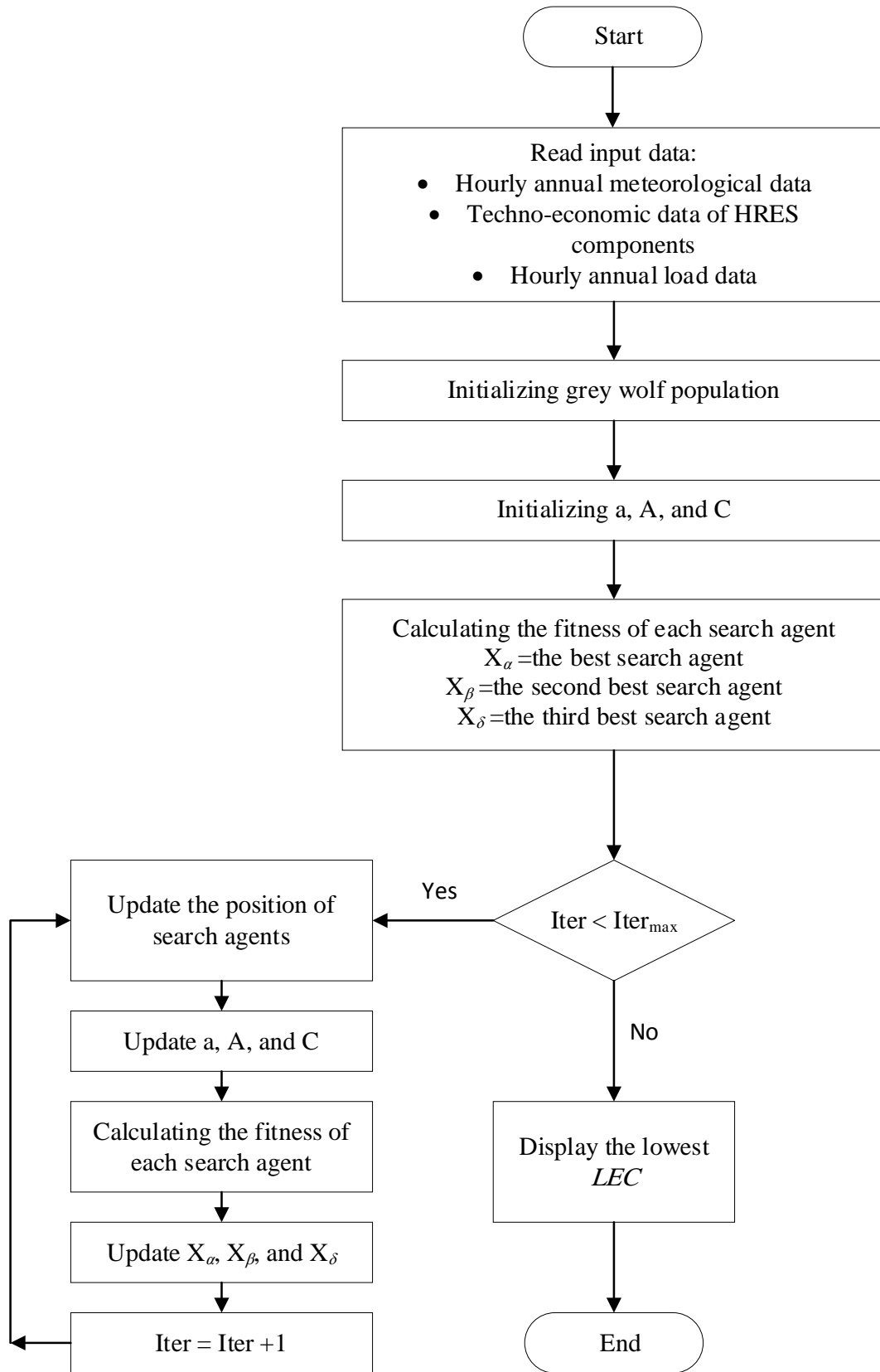


Figure 5: The process of optimization using GWO algorithm

7. The Case Study

In this paper, the proposed CP is used to calculate the optimum size of the proposed hybrid system and supply a load demand at a site located in New Valley Governorate in the southwestern part of Egypt. The site is located in the north of

Dakhla Oasis at (25° 51' 36"N 28° 34' 48"E). The hourly load profile shown in Figure 6 is utilized as a case study. In addition, the real data of the mean annual wind speed at the specific location is approximately 5.08 m/s at 10 m height and the mean horizontal irradiance is 6.05 kWh/m²/day.

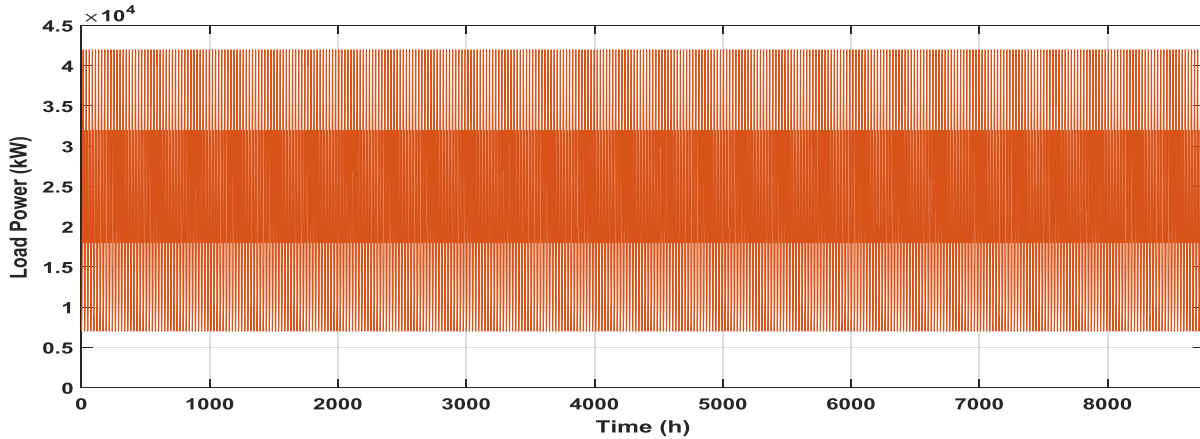


Figure 6: Hourly load profile

Figure 7 depicts the real hourly for the wind speeds data at 10 m height and Figure 8 depicts the solar insolation on the titled PV array surface for the selected location. The optimization section is a fundamental component of the CP, which is developed using

IOT. This section is developed to meet the specific values of the E_{dummy} and $LOLP$ of the proposed HRES. Then, the LEC is calculated to achieve the optimal HRES size and satisfy the load requirements.

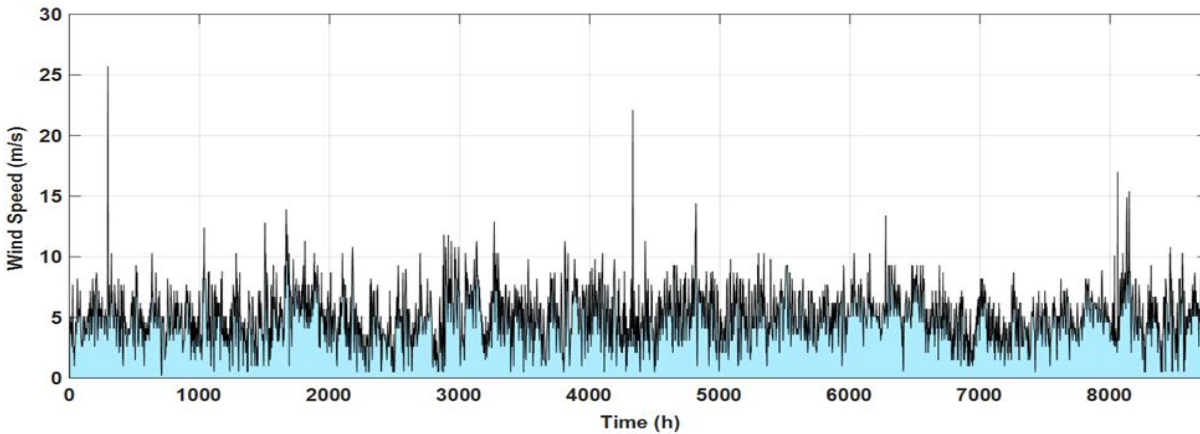


Figure 7: Hourly wind speeds for the selected site

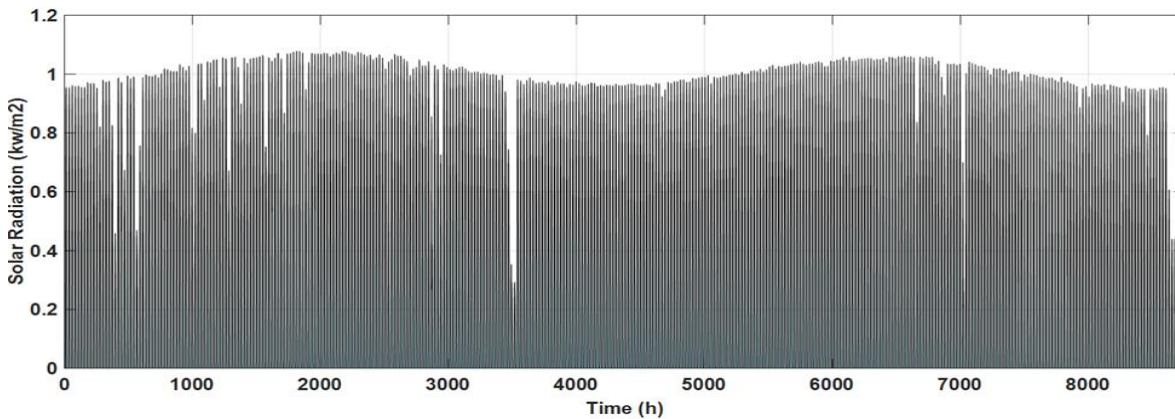


Figure 8: Hourly tilted solar insolation for the selected site

8. Simulation Results and Discussion

The IOT is utilized to calculate the optimum size of the proposed hybrid system to provide a load demand at a site located in New Valley Governorate in the southwestern part of Egypt. The results of simulation clarified that the minimum *LEC* generated from the HRES for the site is obtained using an ITP-1 WTG, and the rated power of the DG, $P_{DG,r}$ used is less than 50% of the peak load. Figure 9 depicts the schematic diagram of proposed model of the HRES components utilized for validation. The HRES components that have been utilized in both the developed IOT and HOMER software are the same.

Figures 10 and 11 depict the first and the final iterations of optimization, respectively, which depict the performance of the optimization sizing process until obtain the optimal solution ITP-1 WTG with a penetration ratio of 35%. The number of iterations relies upon the variables of optimization and constraints. The figures depict the change in the required load, P_L , the power of dummy loads, P_{dummy} , the battery storage accumulated power, P_B , and the power of DG, P_{Dg} , over time until the optimal solution is obtained.

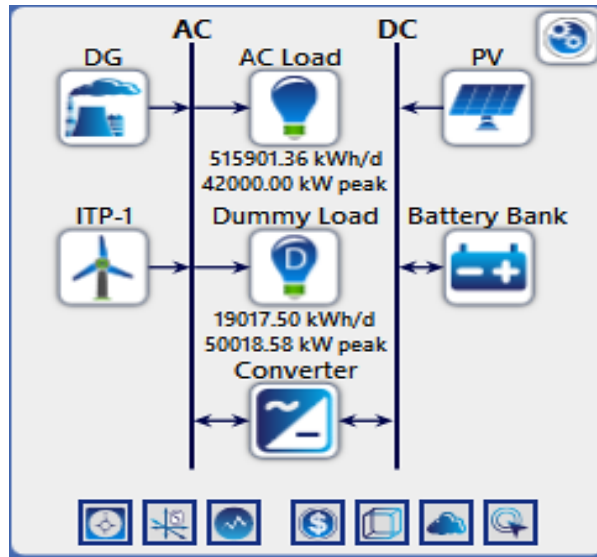


Figure 9: The schematic diagram of the HRES components

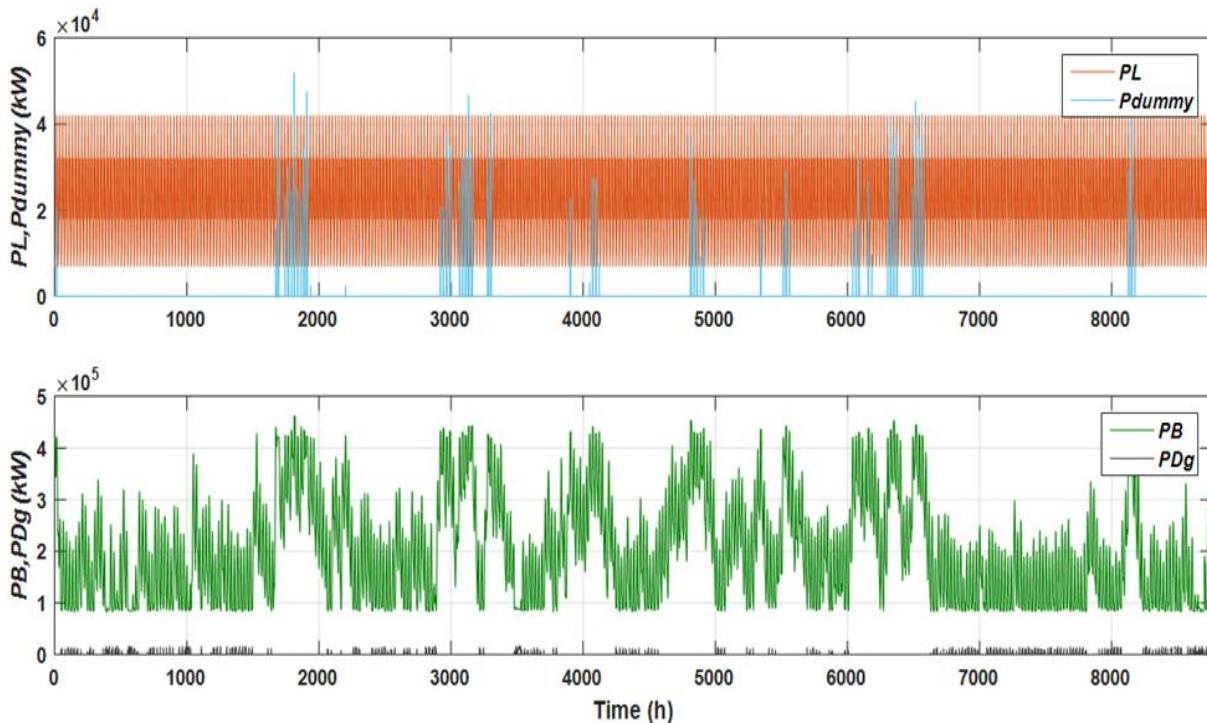


Figure 10: The first iteration of sizing optimization

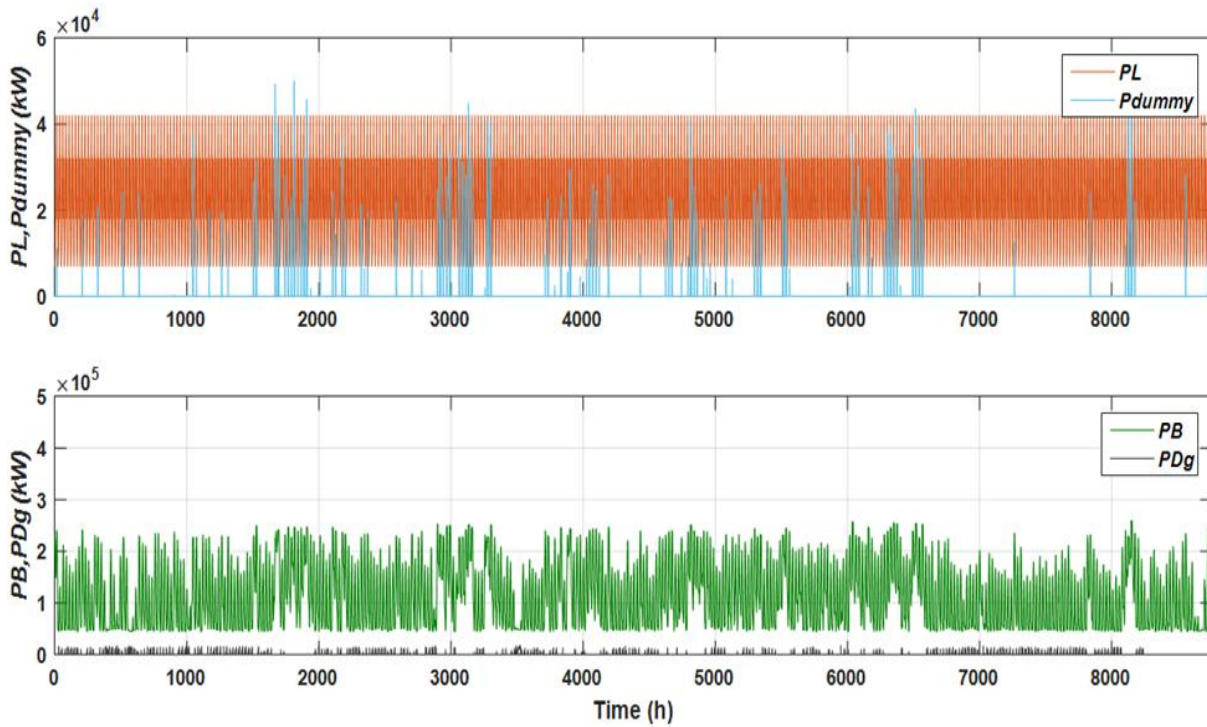


Figure 11: The final iteration of sizing optimization

Figure 12 shows the change in power per hour for a period of one year for the proposed HRES components in the optimal case. In this figure, the simulation outcomes are presented as: the required load (P_L), the total power provided by RES ($P_W + P_{PV}$), the battery storage system charging and discharging power (P_{BC}

& P_{BD}), the power of DG (P_{Dg}) and the power of dummy load (P_{dummy}). This figure shows the DG is in operation during the time when insufficient renewable energy is produced, and the storage batteries are not able to provide unsatisfactory loads.

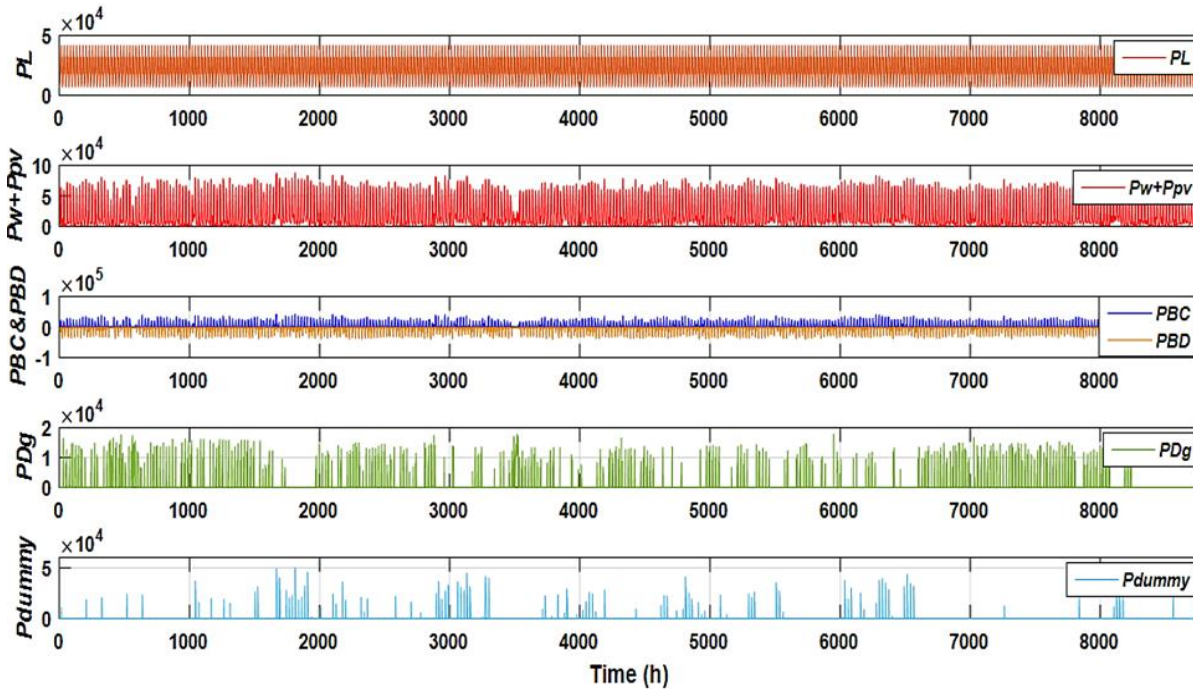


Figure 12: Hourly results of simulation in the optimal case

The results of simulation for a certain 24-hour in the optimal case is shown in Figure 13 which illustrates the change in the power of load (P_L), the power obtained from the WTG and PV systems ($P_W + P_{PV}$), and the output power obtained from the DG

(P_{Dg}) of a specific 24 hours of the one year to act as an illustration for more recognizing the logic used by the proposed optimization algorithm.

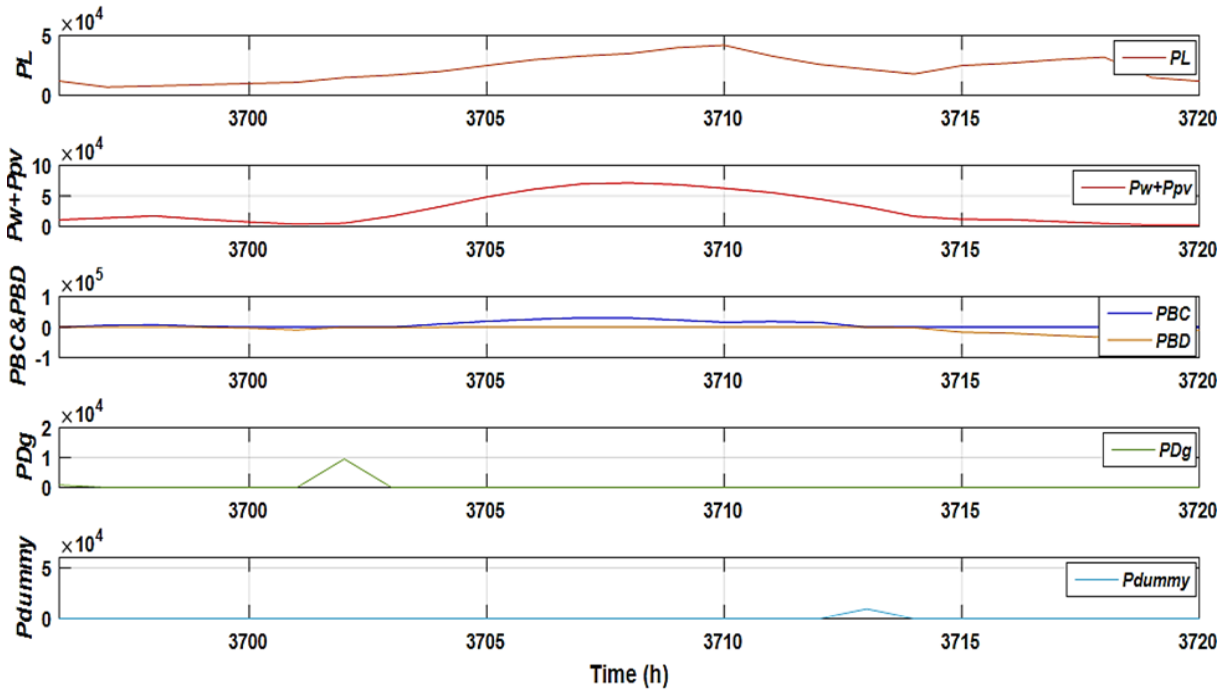


Figure 13: Results of simulation for a certain 24 hours in the optimal case

Table 3 demonstrates the values of LEC for the specific location with the penetration ratio for each WTG in the case study. In this Table, it can be noted that the lowest value of the LEC is achieved at a 35% penetration ratio with ITP-1 WTG.

Figure 14 shows the changing in the LEC versus the penetration ratio in the optimal case. In the optimum case, the contribution from the WTG and PV systems are at 35% penetration ($N_{WTG} = 85$ WTG, $A_{PV} = 6.84 \times 10^5 \text{ m}^2$).

Table 3: The LEC values with the penetration ratio per each WTG in the case study

penetration	Fuhrlander-3	Ecotecnia-2	ITP-1	NEPC-3	Enercon-2
0.05	0.221	0.222	0.217	0.221	0.218
0.1	0.217	0.218	0.214	0.221	0.216
0.15	0.214	0.217	0.210	0.220	0.211
0.2	0.213	0.214	0.204	0.221	0.207
0.25	0.210	0.218	0.201	0.221	0.208
0.3	0.208	0.216	0.198	0.225	0.203
0.35	0.209	0.242	0.196	0.260	0.205
0.4	0.228	0.259	0.200	0.249	0.215
0.45	0.237	0.243	0.221	0.251	0.231
0.5	0.237	0.244	0.220	0.252	0.230
0.55	0.238	0.244	0.219	0.251	0.230
0.6	0.240	0.244	0.220	0.250	0.229
0.65	0.240	0.243	0.220	0.255	0.229
0.7	0.238	0.243	0.219	0.249	0.228
0.75	0.237	0.242	0.219	0.248	0.227
0.8	0.235	0.242	0.218	0.248	0.227
0.85	0.234	0.242	0.217	0.247	0.227
0.9	0.233	0.241	0.216	0.246	0.226
0.95	0.232	0.241	0.215	0.246	0.226

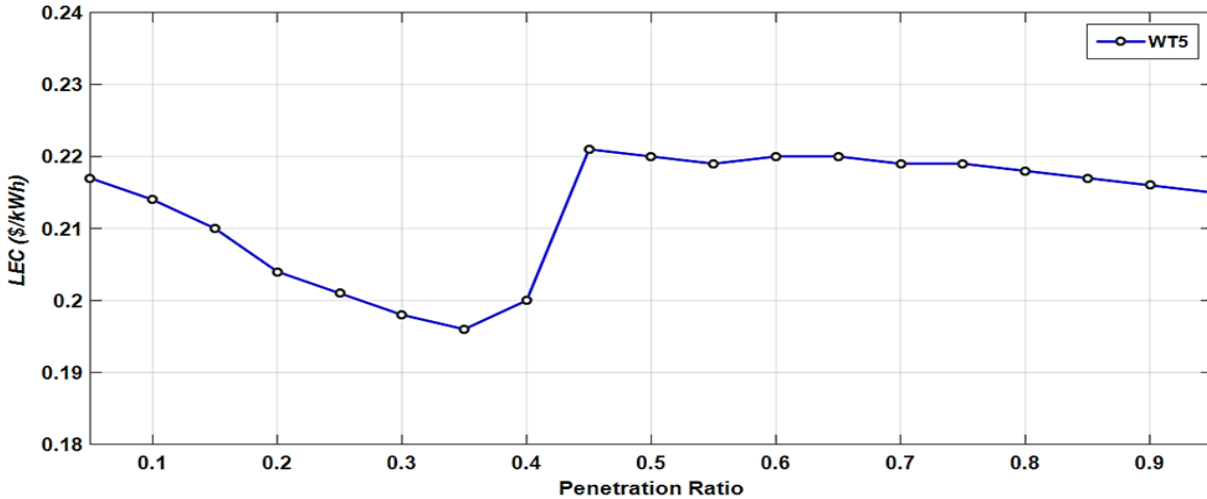


Figure 14: Change of LEC versus the penetration ratio for ITP-1 WTG

The simulation results obtained from the mathematical model and CP based on IOT are validated against HOMER software and GWO for the HRES shown in Figure 1 of the selected site is introduced. For the purposes of validation, the HRES components

that have been utilized in the developed IOT, HOMER and GWO are the same. The detailed optimization results for the selected site using HOMER software are shown in Figure 15.

Architecture										Cost			System	
PV (kW)	ITP-1	DG (kW)	Battery Bank	Converter (kW)	Dispatch	NPC (\$)	COE (\$)	Operating cost (\$/yr)	Initial capital (\$)	Ren. Frac (%)	Total f (L/y)			
139,300	86	17,858	288,916	36,364	LF	\$685M	\$0.206	\$20.0M	\$344M	97.1	3,110,			
141,153	91	17,858	292,102	37,226	LF	\$686M	\$0.206	\$19.7M	\$350M	97.5	2,727,			
128,334	168	17,858	233,778	31,307	LF	\$687M	\$0.207	\$19.8M	\$349M	95.6	4,433,			
130,236	169	17,858	233,200	32,328	LF	\$687M	\$0.207	\$19.6M	\$353M	96.0	4,153,			
138,648	89	17,858	286,693	34,539	LF	\$688M	\$0.207	\$20.3M	\$343M	96.8	3,451,			
143,197	100	17,858	289,171	38,236	LF	\$688M	\$0.207	\$19.5M	\$357M	97.8	2,365,			
126,805	174	17,858	233,383	31,054	LF	\$689M	\$0.207	\$19.9M	\$349M	95.5	4,451,			
137,423	110	17,858	289,262	35,661	LF	\$689M	\$0.207	\$19.8M	\$351M	97.5	2,670,			
128,326	171	17,858	230,156	30,939	LF	\$689M	\$0.207	\$19.9M	\$350M	95.4	4,611,			
141,146	98	17,858	288,163	35,452	LF	\$690M	\$0.207	\$19.8M	\$352M	97.3	2,898,			
134,678	103	17,858	291,145	33,593	LF	\$690M	\$0.207	\$20.3M	\$344M	97.0	3,301,			
124,819	171	17,858	236,128	30,170	LF	\$690M	\$0.207	\$20.2M	\$345M	95.2	4,751,			
141,579	78	17,858	293,175	36,261	LF	\$691M	\$0.208	\$20.3M	\$345M	97.1	3,165,			
139,876	77	17,858	291,664	35,008	LF	\$691M	\$0.208	\$20.6M	\$341M	96.7	3,474,			
126,530	183	17,858	230,553	30,801	LF	\$692M	\$0.208	\$19.9M	\$352M	95.6	4,438,			

Figure 15: The optimization results HOMER software

The comparison between the results for the specific site is depicted in Table 4. It can be observed that the results acquired from the IOT, HOMER, and GWO have a great agreement. The CP using IOT can optimize the size of each HRES component relying upon the minimum LEC. HOMER software requires the modeler to input several possible choices for each component of the system to obtain the best choice from these choices which represent as a major limitation of HOMER. Therefore, the minimum cost acquired by HOMER is not the optimal solution

however it will be the best possible choice from all the obtainable choices introduced as an input data for system components. The grey wolf population has been set to be 30 search agents, and the maximum number of iterations of the GWO was implemented to be 100. The lowest LEC acquired from GWO compared to IOT and HOMER is more accurate as GWO ensures that it meets the constraints of optimization and the objective function. The GWO is capable of obtaining the global optimal with relative simple computational requirements and faster convergence.

Table 4: The comparison between the results for the selected site

Tools	NWTG	APV	IC	RC	OMC	FC	PVS	LEC	No. of Iterations
IOT	85	6.84×10^5	3.32×10^8	2.06×10^8	8.64×10^7	1.07×10^8	-7.1×10^7	0.196	623
Cost %			50.031	31.15	13.1	16.24	-10.7		
HOMER	86	6.83×10^5	3.44×10^8	2.32×10^8	9.3×10^7	4.2×10^7	-2.6×10^7	0.206	
Cost %			50.02	33.94	13.58	6.19	-3.86		
GWO	84	6.88×10^5	3.29×10^8	1.94×10^8	8.46×10^7	1.07×10^8	-6.8×10^7	0.192	< 20
Cost %			50.86	29.97	13.07	16.58	-10.49		

Figure 16 depicts the convergence curve of the GWO algorithm meanwhile obtaining the minimum LEC generated from the system for 5 independent trials. In this figure it can be observed the optimal solution is converged after about 20

iterations, and 100 iterations can be considered as an acceptable end measure. Moreover, the optimal solution converges towards almost the same optimal value (global minima) for all autonomous trials.

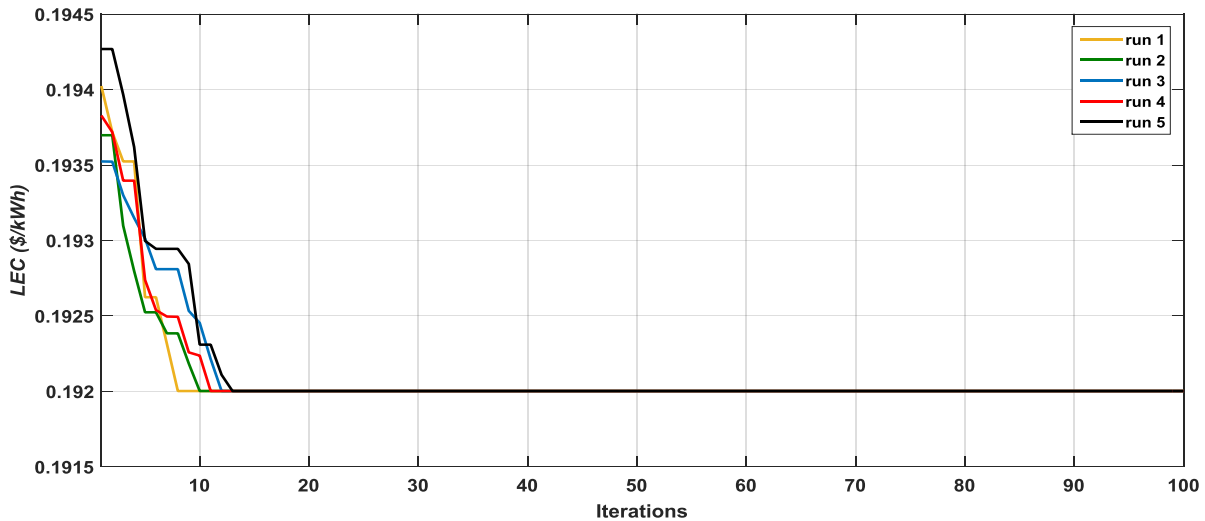


Figure 16: the convergence curve of the GWO algorithm

From Table 4, it can be seen that the IC is the most costly component in the total present value of the overall system. The energy generated from the HRES components for IOT and GWO is shown in Figure 17. As shown in this figure, for using IOT the energy contributions from PV, WTG and DG are 80%, 16%, 4%, respectively with 85 WTG, $6.84 \times 10^5 \text{ m}^2 \text{ APV}$ while for HOMER

software the energy contributions from PV, WTG and DG are 83%, 15%, 2%, respectively with 86 WTG, $6.83 \times 10^5 \text{ m}^2 \text{ APV}$ and finally for implementing GWO the energy contributions from PV, WTG and DG are 81%, 15%, 4%, respectively with 84 WTG, $6.88 \times 10^5 \text{ m}^2 \text{ APV}$.

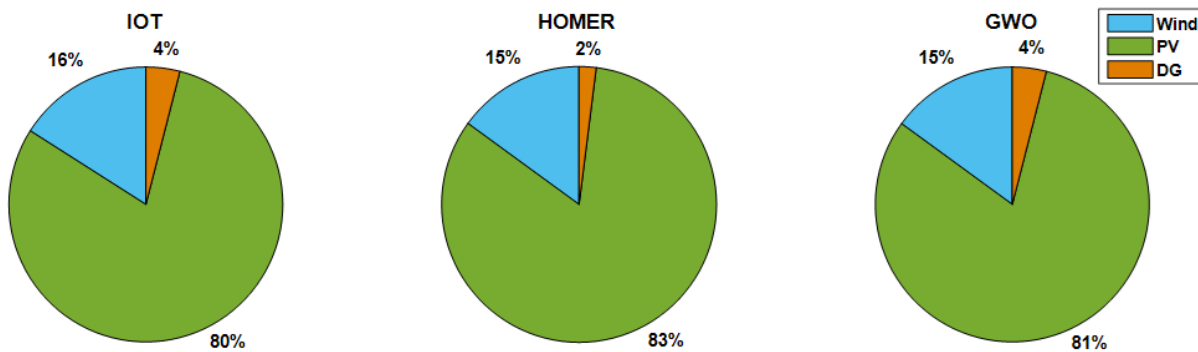


Figure 17: The energy produced by the HRES from IOT and GWO

Generally, in the whole stochastic optimization algorithms inherit random properties. Therefore, the performance of these

algorithms cannot be assessed by just one run. Likewise, the effectiveness and performance of GWO, a newer stochastic

algorithm, is judged via several runs. The level of consistency or robustness of the GWO algorithm for the selected test system is depicting in Figure 14.

9. Conclusion

A methodology for calculating the optimum size of an autonomous PV, wind, battery, DG hybrid power system utilizing IOT is introduced in this paper. The main goal of proposed optimization technique is to calculate the optimal system that satisfies the required load with the lowest *LEC* and the maximum reliability. The results of simulation demonstrated that the proposed optimization technique can obtain the optimal solution and change the variables of optimization under the specific constraints. In addition, this optimization technique can be utilized for any location in the world and for any WTG. The obtained simulation results indicated that the best WTG for the selected location is ITP-1 WTG. Moreover, the best annual contribution from RES is 35% of the WTG and 65% of the PV systems with 85 WTG, $6.84 \times 10^5 \text{ m}^2 \text{ APV}$ and the minimum *LEC* obtained is US\$ 0.196 /kWh. The data acquired from IOT were compared with the outcomes acquired by HOMER software and GWO. The comparison demonstrates the effectiveness of IOT in determining the optimal size of HRES parts.

References

- [1] Mohamed, M. A., Eltamaly, A. M., & Alolah, A. I. Sizing and techno-economic analysis of stand-alone hybrid photovoltaic/wind/diesel/battery power generation systems. *Journal of Renewable and Sustainable Energy*, 7(6), 063128, 2015.
- [2] Eltamaly, A. M., Addoweesh, K. E., Bawah, U., & Mohamed, M. A. New software for hybrid renewable energy assessment for ten locations in Saudi Arabia. *Journal of Renewable and Sustainable Energy*, 5(3), 033126, 2013.
- [3] He, Y., Guo, S., Zhou, J., Ye, J., Huang, J., Zheng, K., & Du, X. Multi-objective planning-operation co-optimization of renewable energy system with hybrid energy storages. *Renewable Energy*, 184, 776-790, 2022.
- [4] Khezri, R., Mahmoudi, A., Aki, H., & Muyeen, S. M.. Optimal Planning of Remote Area Electricity Supply Systems: Comprehensive Review, Recent Developments and Future Scopes. *Energies*, 14(18), 5900, 2021.
- [5] Cuisinier, E., Bourasseau, C., Ruby, A., Lemaire, P., & Penz, B. Techno-economic planning of local energy systems through optimization models: a survey of current methods. *International Journal of Energy Research*, 45(4), 4888-4931, 2021.
- [6] E. R. Shouman, E. El Shenawy, and N. Khattab, "Market financial analysis and cost performance for photovoltaic technology through international and national perspective with case study for Egypt," *Renewable and Sustainable Energy Reviews*, vol. 57, pp. 540-549, 2016.
- [7] M. A. El-Sayed, "Substitution potential of wind energy in Egypt," *Energy Policy*, vol. 30, pp. 681-687, 2002.
- [8] Eltamaly, A. M., & Mohamed, M. A. A novel software for design and optimization of hybrid power systems. *Journal of the Brazilian Society of Mechanical Sciences and Engineering*, 38(4), 1299-1315, 2016.
- [9] Mohamed, M. A., Eltamaly, A. M., & Alolah, A. I. PSO-based smart grid application for sizing and optimization of hybrid renewable energy systems. *PloS one*, 11(8), e0159702, 2016.
- [10] H. Yang, W. Zhou, L. Lu, and Z. Fang, "Optimal sizing method for stand-alone hybrid solar-wind system with LPSP technology by using genetic algorithm," *Solar energy*, vol. 82, pp. 354-367, 2008.
- [11] S. K. Ramoji and B. J. Kumar, "Optimal economical sizing of a PV-wind hybrid energy system using genetic algorithm and teaching learning based optimization," *International Journal of Advanced Research in Electrical, Electronics and Instrumentation Engineering*, vol. 3, pp. 7352-7367, 2014.
- [12] S. Tafreshi, H. Zamani, S. Ezzati, M. Baghdadi, and H. Vahedi, "Optimal unit sizing of distributed energy resources in microgrid using genetic algorithm," in 2010 18th Iranian Conference on Electrical Engineering, 2010, pp. 836-841.
- [13] H. Yang, L. Lu, and W. Zhou, "A novel optimization sizing model for hybrid solar-wind power generation system," *Solar energy*, vol. 81, pp. 76-84, 2007.
- [14] M. Jayachandran and G. Ravi, "Design and optimization of hybrid micro-grid system," *Energy Procedia*, vol. 117, pp. 95-103, 2017.
- [15] Eltamaly, A. M., Mohamed, M. A., Al-Saud, M. S., & Alolah, A. I. (2017). Load management as a smart grid concept for sizing and designing of hybrid renewable energy systems. *Engineering Optimization*, 49(10), 1813-1828.
- [16] E. M. Mokheimer, A. Al-Sharafi, M. A. Habib, and I. Alzaharnah, "A new study for hybrid PV/wind off-grid power generation systems with the comparison of results from homer," *International Journal of Green Energy*, vol. 12, pp. 526-542, 2015.
- [17] M. A. Mohamed, A. M. Eltamaly, and A. I. Alolah, "Swarm intelligence-based optimization of grid-dependent hybrid renewable energy systems," *Renewable and Sustainable Energy Reviews*, vol. 77, pp. 515-524, 2017.
- [18] M. Bashir and J. Sadeh, "Size optimization of new hybrid stand-alone renewable energy system considering a reliability index," in 2012 11th International conference on environment and electrical engineering, 2012, pp. 989-994.
- [19] M. Combe, A. Mahmoudi, M. H. Haque, and R. Khezri, "AC- coupled hybrid power system optimisation for an Australian remote community," *International Transactions on Electrical Energy Systems*, vol. 30, p. e12503, 2020.
- [20] N. Agarwala, A. Kumarb, and Varun, "Sizing analysis and cost optimization of hybrid solar-diesel-battery based electric power generation system using simulated annealing technique," *Distributed Generation & Alternative Energy Journal*, vol. 27, pp. 26-51, 2012.
- [21] R. Chedid and S. Rahman, "Unit sizing and control of hybrid wind-solar power systems," *IEEE Transactions on energy conversion*, vol. 12, pp. 79-85, 1997.
- [22] A. Yahiaoui, F. Fodhil, K. Benmansour, M. Tadjine, and N. Cheggaga, "Grey wolf optimizer for optimal design of hybrid renewable energy system PV-Diesel Generator-Battery: Application to the case of Djanet city of Algeria," *Solar Energy*, vol. 158, pp. 941-951, 2017.

[23] L. I. Wong, M. Sulaiman, M. Mohamed, and M. S. Hong, "Grey Wolf Optimizer for solving economic dispatch problems," in 2014 IEEE international conference on power and energy (PECon), 2014, pp. 150-154.

[24] V. K. Kamboj, S. Bath, and J. Dhillon, "Solution of non-convex economic load dispatch problem using Grey Wolf Optimizer," *Neural computing and Applications*, vol. 27, pp. 1301-1316, 2016.

[25] A. M. Yasin, "Optimum Design of a Stand-alone Hybrid Energy System for a Remote Village in Palestinian Territories," *Journal of Engineering Research and Technology*, vol. 4, 2017.

[26] S. K. Nandi and H. R. Ghosh, "A wind-PV-battery hybrid power system at Sitakunda in Bangladesh," *Energy Policy*, vol. 37, pp. 3659-3664, 2009.

[27] A. M. Eltamaly, M. A. Mohamed, and A. I. Alolah, "A novel smart grid theory for optimal sizing of hybrid renewable energy systems," *Solar Energy*, vol. 124, pp. 26-38, 2016.

[28] G. M. Masters, *Renewable and efficient electric power systems*: John Wiley & Sons, 2013.

[29] A. M. Eltamaly and M. A. Mohamed, "A novel design and optimization software for autonomous PV/wind/battery hybrid power systems," *Mathematical Problems in Engineering*, vol. 2014, 2014.

[30] T.-H. Yeh and L. Wang, "A study on generator capacity for wind turbines under various tower heights and rated wind speeds using Weibull distribution," *IEEE Transactions on Energy Conversion*, vol. 23, pp. 592-602, 2008.

[31] J. L. Bernal-Agustín and R. Dufo-Lopez, "Simulation and optimization of stand-alone hybrid renewable energy systems," *Renewable and sustainable energy reviews*, vol. 13, pp. 2111-2118, 2009.

[32] E. Sreeraj, K. Chatterjee, and S. Bandyopadhyay, "Design of isolated renewable hybrid power systems," *Solar Energy*, vol. 84, pp. 1124-1136, 2010.

[33] I. Y. Lun and J. C. Lam, "A study of Weibull parameters using long-term wind observations," *Renewable energy*, vol. 20, pp. 145-153, 2000.

[34] R. Belfkira, P. Reghem, J. Raharijaona, G. Barakat, and C. Nichita, "Non linear optimization based design methodology of wind/PV hybrid stand alone system," *Proceedings of the European Association for Vision and Eye Research (EVER'09)*, vol. 1, pp. 1-7, 2009.

[35] M. S. Ismail, M. Moghavvemi, and T. Mahlia, "Techno-economic analysis of an optimized photovoltaic and diesel generator hybrid power system for remote houses in a tropical climate," *Energy conversion and management*, vol. 69, pp. 163-173, 2013.

[36] R. Dufo-López, J. L. Bernal-Agustín, J. M. Yusta-Loyo, J. A. Domínguez-Navarro, I. J. Ramírez-Rosado, J. Lujano, et al., "Multi-objective optimization minimizing cost and life cycle emissions of stand-alone PV-wind-diesel systems with batteries storage," *Applied Energy*, vol. 88, pp. 4033-4041, 2011.

[37] P. Nema, R. Nema, and S. Rangnekar, "A current and future state of art development of hybrid energy system using wind and PV-solar: A review," *Renewable and Sustainable Energy Reviews*, vol. 13, pp. 2096-2103, 2009.

[38] Focusconomics. (July 29). Interest Rate in Egypt. Available: <https://www.focus-economics.com/country-indicator/egypt/interest-rate>

[39] Egypt Inflation Rate. (July 29). Trading Economics. Available: <http://www.tradingeconomics.com/egypt/inflation-cpi>

[40] A. M. Eltamaly and M. A. Mohamed, "Optimal sizing and designing of hybrid renewable energy systems in smart grid applications," in *Advances in Renewable Energies and Power Technologies*, ed: Elsevier, 2018, pp. 231-313.

[41] A. Kaabeche and R. Ibtouen, "Techno-economic optimization of hybrid photovoltaic/wind/diesel/battery generation in a stand-alone power system," *Solar Energy*, vol. 103, pp. 171-182, 2014.

[42] POWER SYSTEMS TODAY. (July 29). CATERPILLAR 500 KW Generators For Sale. Available: <https://www.powersystemstoday.com/listings/for-sale/caterpillar/500-kw/generators/153001>

[43] S. Mirjalili, S. M. Mirjalili, and A. Lewis, "Grey wolf optimizer," *Advances in engineering software*, vol. 69, pp. 46-61, 2014.

Nomenclature

Abbreviations

LEC	Levelized energy cost.
IOT	Iterative Optimization Technique.
DG	Diesel generator.
CP	Computer Program.
WTG	Wind turbine generator.
GWO	Grey Wolf Optimizer.
RES	Renewable energy sources.
HRES	Hybrid renewable energy system.
GA	Genetic Algorithm
PSO	Particle Swarm Optimization.
LOLP	Loss of load probability.
STC	Standard test conditions.
Symbols	
SOC	The battery state of charge.
SOCmin	The battery minimum state of charge.
PPV	The output power of the PV system.
Gt	Solar insolation on the inclined surface.
APV	Area of the PV panels.
$\mu_{pv}(t)$	The PV module instantaneous efficiency.
Kt	The temperature coefficient.
μ_{th}	The solar cells theoretical efficiency at STC.
Tnom	The solar cells theoretical temperature at STC.
Tc(t)	The temperature at time t for solar cells.
Tamb	Ambient temperature.
NOCT	Nominal operating cells temperature.
PL-av	The average required load.
SF	The factor of safety.
VF	The factor of variability.
h	The height of the wind turbine hub.
hg	The height of the anemometer.
v(h)	The wind speed at the desired height of the hub.
v(hg)	The wind speed at the anemometer height.
α	The roughness factor.
PW	The power obtained from a wind turbine.
Pr_wt	The rated electrical power generated from a wind turbine generator.
V	The wind speeds.
vc, vr, vf	The cut-in, rated power and cut-off wind speeds, respectively.
K	Shape parameter.

C	Scale parameter.
v_i	Wind speeds at time interval i .
W	Number of non-zero wind speeds.
CF	The capacity factor for wind turbine.
PWT-av	The wind turbine generator average power.
ANWTG	The wind turbines generators average number
C _{bat}	The battery bank stored energy
η_{CH}, η_{DIS}	The battery efficiency during charging and discharging.
σ	The self-discharge rate of battery.
η_{conv}	The efficiency of converter.
C_{bat_min}, C_{bat_max}	Minimum and maximum battery bank allowable capacity
DOD	Maximum depth of discharge.
C_{bat_r}	Battery bank nominal capacity.
F(t)	The DG fuel consumption per hour.
PD _g	The hourly power produced by the DG.
PD _{g_r}	The rated power of the DG.
α_{DG}, β_{DG}	The coefficients of the fuel consumption curve.
NPC	The net present cost.
ARL	The annual required load.
CRF	Capital recovery factor.
Y	The project lifetime.
I	The real net rate of interest.
i'	The annual nominal rate of interest.
F	The annual inflation rate.
IC	Initial capital cost.
CPV	The PV system cost including civil works per kW.
PV _r	The PV array rated power.
CWTG	The WTG cost including civil works per kW.
NWTG	The number of WTG.
CBT	The battery bank cost per kWh.
Pr _{conv}	The rated power of the inverter.
C _{conv}	The inverter cost per kW.
C _{dg}	The cost of DG per kW.
OM	Operation and maintenance costs.
OM(1)	The operating and maintenance costs in the first year.
RC	Replacement cost.
CRC	The replacement components capacity.
CU	The replacement components cost.
NRep	The number of replacements for system components.
FC	The fuel cost of DG.
tdg	The DG overall operation hours during the system life.
P _{fuel}	The price of fuel per liter.
PSV	Present scrap value.
SV	The scrap value of the project components.
E _{dummy}	The energy of dummy load.
PL	The power of load.
P _{dummy}	The power of dummy load.
PBC	The battery storage charging power.
PBD	The battery storage discharging power
PB	Accumulated power of battery.
$\alpha, \beta, \delta, \text{ and } \omega$	Alpha, beta, delta, and omega wolves.
\vec{X}	The grey wolf position vector.
\vec{X}_p	The prey position vector.
t	The current iteration number.
\vec{A}, \vec{C}	The coefficient vectors.
\vec{a}	Linearly decreased vector from 2 to 0.
\vec{r}_1, \vec{r}_2	Random vectors from 0 to 1.